ELSEVIER

Journal of Hazardous Materials A85 (2001) 165–179

Journal of Hazardous Materials

www.elsevier.com/locate/jhazmat

Modelling aerosol processes related to the atmospheric dispersion of sarin

Jaakko Kukkonen [a,*], Kari Riikonen [a], Juha Nikmo [a], Arto Jäppinen [b], Kari Nieminen [b]

[a] *Air Quality Research, Finnish Meteorological Institute, Sahaajankatu 20 E, FIN-00810 Helsinki, Finland*
[b] *Explosives and NBC Defence Section, Defence Forces Research Institute of Technology, Box 5, FIN-34111 Lakiala, Finland*

Received 31 August 2000; received in revised form 28 February 2001; accepted 28 February 2001

Abstract

We have developed mathematical models for evaluating the atmospheric dispersion of selected chemical warfare agents (CWA), including the evaporation and settling of contaminant liquid droplets. The models and numerical results presented may be utilised for designing protection and control measures against the conceivable use of CWA's. The model AERCLOUD (AERosol CLOUD) was extended to treat two nerve agents, sarin and VX, and the mustard agent. This model evaluates the thermodynamical evolution of a five-component aerosol mixture, consisting of two-component droplets together with the surrounding three-component gas. We have performed numerical computations with this model on the evaporation and settling of airborne sarin droplets in characteristic dispersal and atmospheric conditions. In particular, we have evaluated the maximum radii (r_M) of a totally evaporating droplet, in terms of the ambient temperature and contaminant vapour concentration. The radii r_M range from approximately 15–80 μm for sarin droplets for the selected ambient conditions and initial heights. We have also evaluated deposition fractions in terms of the initial droplet size.

Keywords: Chemical warfare agent; CWA; Sarin; Aerosol; Atmospheric dispersion; Model

1. Introduction

The airborne dispersal of a liquefied chemical warfare agent (CWA) results in contaminant liquid droplets of various sizes. Larger contaminant liquid droplets may deposit near the point of release, causing ground contamination. Smaller droplets may remain suspended

* Corresponding author. Tel.: +358-9-1929-5450; fax: +358-9-1929-5403.
E-mail address: jaakko.kukkonen@fmi.fi (J. Kukkonen).

0304-3894/01/$ – see front matter
PII: S0304-3894(01)00195-9

Nomenclature

c	molar density (kmol m^{-3})
C_d	coefficient of drag
C_p	specific heat (J (kg K)$^{-1}$)
d	diameter (m)
D	binary diffusion coefficient (m^2 s^{-1})
$\bar{e}$	heat flux density (J (s m)$^{-1}$)
g	acceleration due to gravity (m s^{-2})
H_v	specific enthalpy (J kg^{-1})
$\bar{i}$	mass flux density (kg (s m)$^{-1}$)
I	mass flux (kg s^{-1})
k	Boltzmann's constant (J K^{-1})
k_g	thermal conductivity (W (m K)$^{-1}$)
M	molecular weight (kg kmol^{-1})
$\bar{n}$	molar flux density (kmol (s m)$^{-1}$)
Nu	Nusselt number
p	pressure (Pa)
P	pressure (atm)
Pr	Prandtl number
Q	heat flux (J s^{-1})
r	radius (m)
Re	Reynolds number
S	saturation ratio
Sc	Schmidt number
Sh	Sherwood number
t	temperature (°C)
T	temperature (K)
v	velocity (m s^{-1})
X	mole fraction

Greek symbols

ε	Lennard–Jones energy (J)
μ	dynamic viscosity (kg (s m)$^{-1}$)
ρ	density (kg m^{-3})
σ	Lennard–Jones length (Å)
Ω	collision integral

as an aerosol, forming a so-called primary cloud, which may be transported in the air over substantial distances. Vaporising contaminant liquid on the ground forms a so-called secondary cloud. For persistent CWA's, a substantial ground contamination is formed, while for volatile agents, most of the contaminant is contained in the primary cloud. Fig. 1 illustrates these processes.

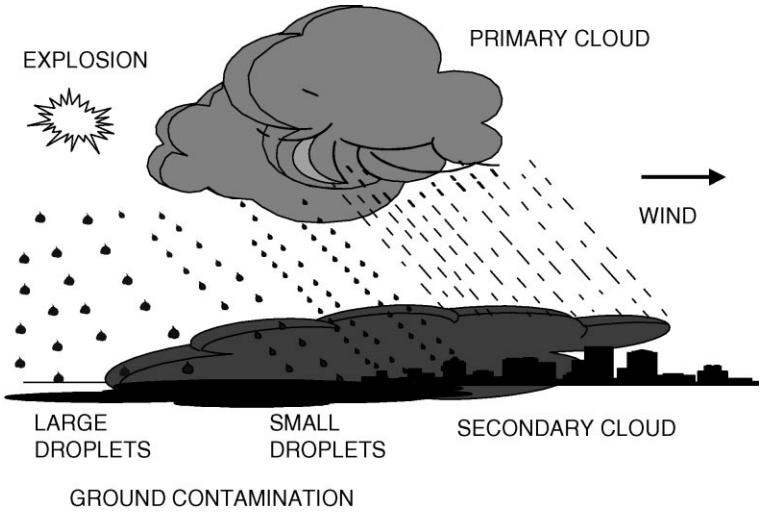

Fig. 1. A schematic diagram of the dispersal and spreading of chemical warfare agents in the atmosphere.

Modelling of these processes requires (i) an estimation of the initial dispersal mechanisms, together with treatments of (ii) the source term evolution, (iii) the dispersion of the primary aerosol cloud, (iv) vaporisation of liquid deposited on the ground, and (v) the subsequent atmospheric dispersion of the secondary cloud. The crucial factors for these processes are the meteorological conditions, aerosol phenomena (particularly the vaporisation and settling of liquid droplets), the chemical and physical properties of the substances, and the ambient terrain and obstacles.

Most of the available literature addresses modelling using various versions of Gaussian models (for example, Milly and Thayer [1], Johnson [2], Somani [3] and Whitacre et al. [4]). Some authors have presented models of the vaporisation and settling of airborne contaminant droplets (for example, Aroesty [5] and Johnson [2]), and of the vaporisation of ground contamination (for example, Johnson [2]). The United States Army [6], for example, utilises mathematical models and results presented by Johnson [2] and Aroesty [5] (the NUSSE2 model), and Somani [3] and Whitacre et al. [4] (the D2PC model). Kolodkin [7] has presented an analysis of the explosions and fires of storehouses containing chemical ammunition composed of organophosphorus agents.

The present authors have previously presented the AERCLOUD model (AERosol CLOUD); a detailed description of the model, including numerical results and evaluation against experimental data has been presented by Kukkonen et al. [8], Vesala and Kukkonen [9] and Nikmo et al. [10]. The model evaluates the thermodynamical evolution of a five-component aerosol mixture, consisting of two-component droplets together with the surrounding three-component gas.

We focus here on the evaluation of aerosol processes that are relevant for the source term formation, atmospheric dispersion and deposition of CWA's. We have performed numerical computations with the AERCLOUD model regarding the evaporation and settling of airborne sarin droplets in characteristic dispersal and atmospheric conditions.

2. Mathematical model

2.1. Overview of the AERCLOUD model

In earlier papers, a model was presented for estimating the evolution of an aerosol containing contaminant droplets, contaminant vapour and dry air (Kukkonen et al. [8], Vesala et al. [11]), and the model was validated against experimental results on a laboratory scale (Vesala et al. [11]). Later, the model was generalised to allow for the effects caused by water vapour in the entrained air (Vesala [12], Vesala and Kukkonen [9]), the experimental validation on a laboratory scale being reported by Vesala [12].

The model was originally designed for a constant mass of air, but it has recently been generalised to admit a time-varying ambient dilution (Nikmo et al. [10]). The AERCLOUD model has also been applied to test the homogeneous equilibium (HE) assumption, in the context of two-phase ammonia clouds released in dry and moist air (Kukkonen et al. [13]). The HE model is commonly adopted in dispersion models of two-phase jets and clouds. For a detailed description of the model, we refer the reader to the above-mentioned papers; however, for convenience we present here the main points of the model.

2.2. Expressions for mass and heat transfer

The AERCLOUD model takes account of the detailed temperature and concentration gradients near the surface of a binary droplet. The essential problem is the modelling of the mass and heat transfer processes from the droplets into the surrounding gas. The droplets are assumed to be in the continuum regime and the droplet growth and evaporation are assumed to be quasistationary, i.e. the droplets are large enough (>1 μm) to see the surrounding gas as a continuum, and the concentration and temperature profiles around the droplets are at any time essentially the same as in the steady state, with changes directly following changes in the boundary conditions.

The mass fluxes are calculated using the well-known formula taking into account ordinary diffusion; thermal diffusion resulting from the temperature gradient is ignored (see Kulmala and Vesala [14]). The influence of forced convection (due to the free fall of droplets) shall be addressed later. For a n-component ideal vapour mixture the mole fraction gradient of the species i due to ordinary diffusion, ∇X_i, is given by the Stefan–Maxwell equations (Curtiss and Hirschfelder [15]):

$$\nabla X_i = \sum_{j=1,\, j\neq i}^{n} (cD_{ij})^{-1}(X_i \bar{n}_j - X_j \bar{n}_i) \tag{1}$$

where c is the molar density of the mixture, D_{ij} the diffusion coefficient for the pair i–j in a binary mixture, i.e. the binary diffusion coefficient of species i with respect to species j and $\bar{n}_i$ the molar flux density of species i in the stationary coordinates.

In the present model, we consider binary vapour mass transfer in an inert gas. There is no net flux of the inert gas in the stationary coordinates, and its molar flux density vanishes. The Stefan–Maxwell equations form therefore for this system a set of two non-linear differential equations for the vapour mole fractions. This set of differential equations can be solved

analytically, which produces non-linear algebraic equations. The detailed form of these equations has been presented by Vesala and Kukkonen [9].

The heat flux is governed by Fourier's law of heat conduction and by the enthalpy carried by diffusing species. The heat flux density in stationary coordinates is given by (for instance, Bird et al. [16])

$$\bar{e} = -k_{\mathrm{g}} \nabla T + \sum_{j=1}^{n} H_{j\mathrm{v}} \bar{i}_j + \bar{e}_{\mathrm{rad}} \tag{2}$$

where k_{g} is the thermal conductivity of the gas, T the temperature and $H_{j\mathrm{v}}$ the partial specific enthalpy of the vapour of species j. The partial enthalpy of mixing of the gaseous phases can be neglected, and $H_{j\mathrm{v}}$ is therefore equal to the vapour enthalpy of pure species j; $\bar{i}_j$ is the mass flux density of species j and $\bar{e}_{\mathrm{rad}}$ is the radiative heat flux density.

The first term represents pure thermal conduction and it corresponds to the well-known Fourier's law of heat conduction. The second term is the heat transported by diffusion, as a result of the difference in the enthalpies of the diffusing substances. An equation for the temperature of the droplet can be derived using the energy conservation and Eq. (2); the detailed expression has been presented by Vesala and Kukkonen [9].

2.3. The influence of forced convection and the droplet population

If the droplets are moving with respect to the surrounding gas, the rates of mass and heat transfer are increased due to forced convection. If droplet ventilation is allowed for, the diffusive mass fluxes are multiplied by the droplet Sherwood number, and the thermal conductivity is multiplied by the droplet Nusselt number. The Sherwood number is defined as the ratio of the total mass transfer to the purely diffusive mass transfer, and the Nusselt number as the ratio of the total heat flux to the purely conductive heat flux. The following semi-empirical relations were used:

$$Sh = I/I_{\mathrm{d}} = 1 + 0.276\, Re^{1/2} Sc^{1/3} \tag{3}$$

and

$$Nu = Q/Q_{\mathrm{c}} = 1 + 0.276\, Re^{1/2} Pr^{1/3} \tag{4}$$

where I and Q are the total mass and heat fluxes, and I_{d} and Q_{c} are the purely diffusive and conductive fluxes. Droplet Reynolds number $Re = v d_{\mathrm{p}} \rho_{\mathrm{g}} / \mu_{\mathrm{g}}$, where v is the relative velocity of particles and gas, d_{p} the droplet diameter, and ρ_{g} and μ_{g} the density and the dynamic viscosity of the gas, respectively. Schmidt number $Sc = \mu_{\mathrm{g}}/(\rho_{\mathrm{g}} D)$, where D is the binary diffusion coefficient of vapour through air. Prandtl number $Pr = C_{p\mathrm{g}}\, \mu_{\mathrm{g}}/k_{\mathrm{g}}$, where $C_{p\mathrm{g}}$ is the specific heat of the gas.

The terminal settling velocities of droplets (required for the computation of Re) were determined numerically from standard equations. For particles in the continuum regime

$$v = \left(\frac{4 \rho_{\mathrm{d}} d_{\mathrm{p}} g}{3 C_{\mathrm{d}} \rho_{\mathrm{g}}} \right)^{1/2} \tag{5}$$

where ρ_d is the density of the droplet, g the acceleration of gravity and C_d is the coefficient of drag. We utilised the form of the coefficient C_d for various flow regimes in terms of Re presented by Seinfeld [17].

The earlier model version (Vesala and Kukkonen [9]) allowed for the simultaneous evaporation and condensation of a population of droplets, according to the theory presented by Wagner and Pohl [18]. The present model version (Nikmo et al. [10]) uses an extension of this theory. We consider a sphere around a droplet which is substantially larger than the radius of the droplet, but sufficiently small compared with the mean droplet separation. It is assumed that steep vapour pressure and temperature profiles occur only in the immediate vicinity of the droplets, i.e. within the sphere defined above.

Consequently, average vapour pressures and temperatures in the gas (sufficiently far from the droplets) can be defined, and these are then influenced by the entrainment of moist air and by evaporation and condensation processes. The theory is valid at all but the very highest droplet densities. This situation is not expected to be a severe restriction for dispersing clouds.

2.4. The utilisation of the model

In summary, the AERCLOUD model evaluates the thermodynamical evolution of a five-component aerosol mixture. The gas phase consists of an inert gas (such as air) and the vapours of the species forming the droplets. The model also allows for a temporally varying amount of moist air, i.e. entrainment. The model can be utilized as a thermodynamic submodel in heavier-than-air cloud dispersion models. In addition to the thermodynamic evolution, the model also evaluates the contaminant mass deposited as liquid.

3. Numerical results

We present in the following a compilation of the substance properties of the selected CWA's, and results on the evolution of airborne sarin droplets, computed with the AERCLOUD model. The range of conditions selected for the numerical computations is fairly limited, e.g. the release height varies from 1 to 10 m, and the ambient temperature from −20 to +20°C. However, the main objective here is to illustrate the main physical dependencies, not to include all conceivable conditions.

3.1. The relevant physical and chemical properties of sarin, mustard agent and VX

A compilation of the relevant substance properties is presented in Appendix A. These properties were applied in the numerical computations. Sarin and VX are classified as nerve gases; mustard agent is commonly classified as a blister agent.

The saturated vapour pressure is a key parameter in terms of the agent volatility, and the formation and persistence of ground contamination. The vapour pressures of water, sarin, mustard agent and VX have therefore been presented in Fig. 2. All of these CWA's are more persistent than water; sarin is clearly the most volatile of these CWA's, and VX is the most

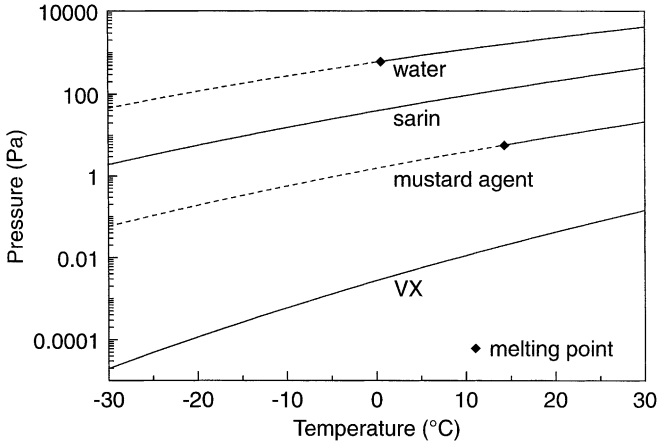

Fig. 2. Variation of the saturated vapour pressure of water, sarin, mustard agent and VX with temperature. The melting points of sarin, mustard agent and VX are −57, +14 and −39°C, respectively (shown in the figure with a diamond).

persistent. Usually sarin is classified as a volatile agent, mustard agent and VX as persistent agents (e.g. Ivarsson et al. [19]).

3.2. The vaporisation and settling of sarin droplets in the atmosphere

Due to relatively high volatility of sarin, both an initial cloud from vaporisation and an evaporation cloud from a ground deposit may result (Milly and Thayer [1]). It is therefore essential to evaluate the vaporisation and deposition of sarin droplets in characteristic dispersal conditions.

Fig. 3 shows the effect of gas temperature on the rate of evaporation of airborne sarin droplets. The concentration of sarin vapour within the cloud is assumed negligible (contaminant saturation ratio in the gas $S = 0$). The rate of the evaporation process increases with increasing gas temperature. Physically, if the gas temperature is low, the processes transferring heat to the droplet surface act more slowly, and drying times are longer.

Fig. 4 shows the drying times of sarin and water droplets for various initial droplet radii. The boiling and melting points of sarin at atmospheric pressure are approximately 152 and −57°C, respectively. The drying times for sarin droplets are longer than those for water droplets, due to the lower volatility of sarin (cf. Fig. 2). The ratio of the corresponding evaporation times for sarin and water varies from 1.8 to 2.4 in the assumed ambient conditions.

The saturation ratios in Fig. 4 for sarin correspond to contaminant concentrations as follows: 0.0012 (+20°C) corresponds to 14 mg m^{-3}, 0.06 (+20°C) corresponds to 714 mg m^{-3} and 0.06 (−20°C) corresponds to 23 mg m^{-3}. The saturation ratio has a very slight influence on droplet evaporation; this is physically caused by the relatively low contaminant vapour pressure compared with the total vapour pressure ($S \ll 1.0$).

In order to estimate the fraction of dispersed material forming ground contamination, it is essential to evaluate the deposition of the droplets. We therefore define a droplet radius

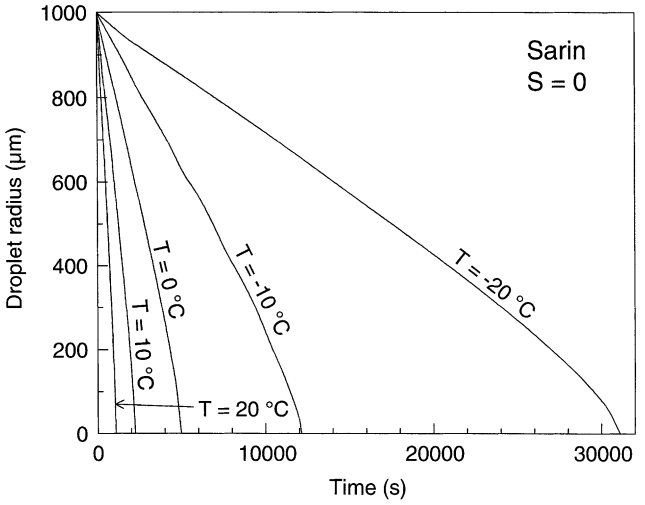

Fig. 3. The effect of gas temperature on the evaporation of a freely-falling sarin droplet. The contaminant saturation ratio of sarin in the gas (S) is negligible.

r_M, for which the drying time (total evaporation time) and the gravitational settling time are equal (Kukkonen et al. [8]). This radius gives the largest totally-evaporating droplet released from a specified height. The radius r_M is a useful concept in deposition estimates. Droplets that are smaller than this size will evaporate totally while still airborne, whereas larger droplets will deposit on the ground before total evaporation takes place.

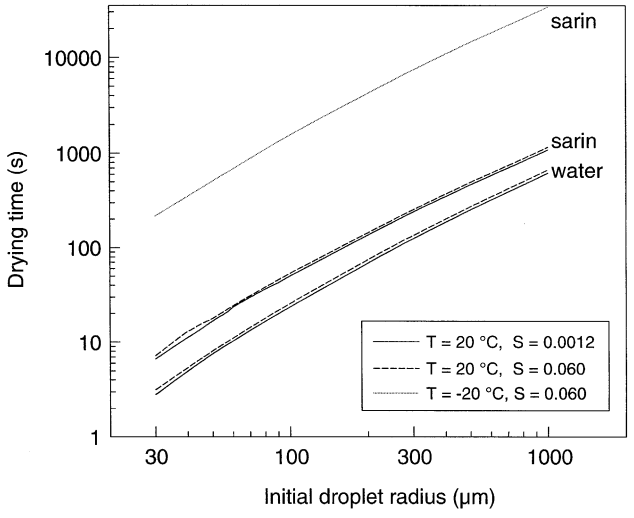

Fig. 4. Variation of the drying time of sarin and water droplets with droplet radius. The curves are shown for three combinations of gas temperature (T) and saturation ratio in the gas (S).

We have assumed here that the gas is at rest, and therefore, the possible instability of droplets in the actual flow field, as well as turbulent deposition, have been neglected. Estimates of liquid deposition using this concept are also possible without using a complex aerosol cloud model; Kukkonen et al. [8] have presented an analytical expression for r_M under simplifying assumptions.

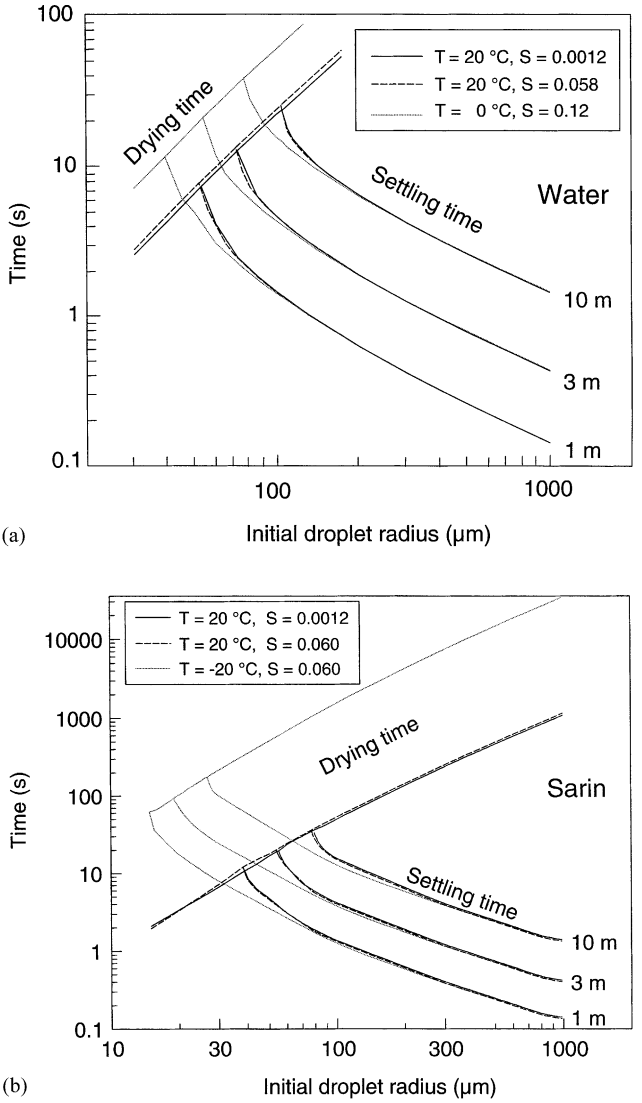

Fig. 5. (a–b) Variation of the drying time and gravitational settling time of water and sarin droplets with initial droplet radius. The curves are shown for three combinations of gas temperature (T) and saturation ratio (S), and the initial height of the droplets ranges from 1 to 10 m.

Fig. 5a–b show the drying and settling times of water and sarin droplets against the droplet radius. The curves have been shown for three combinations of gas temperatures and saturation ratios in the gas, and for three initial heights. The simultaneous evaporation and settling of the droplets have been taken into account in the computation of the curves.

Each settling time curve corresponds to one drying time curve and each intersection point of these curves corresponds to the maximum radius r_M of a totally evaporating droplet. The radii r_M range from approximately 40–110 μm for water droplets for the selected ambient conditions and initial heights. The corresponding radii for sarin droplets range from 15 to 80 μm. The smaller radii for sarin droplets are mainly due to the longer drying times. Evidently, the radius r_M increases with increasing release height, as the gravitational settling time increases with height. For a given release height, r_M decreases with decreasing gas temperature and increasing saturation ratio, as the drying time is longer in these conditions.

The droplet size regimes in which deposition or total evaporation is likely to take place in various conditions can be estimated from Fig. 5b. For instance, for a 100 μm droplet released from heights <10 m in the given conditions, the settling times are less than about 20 s and the drying times are >50 s. The deposited mass fraction is therefore expected to be close to unity.

The above-mentioned curves have been computed assuming a negligible droplet concentration. The effect of the simultaneous evaporation of a population of droplets is to increase the drying times, resulting in smaller r_M; this effect is allowed for in the AERCLOUD model.

As discussed earlier, estimation of the deposition of droplets is important for atmospheric dispersion analyses. We define the deposited mass fraction as the ratio of the deposited contaminant liquid mass to the total contaminant mass (the deposition of vapour is not considered here). Fig. 6 shows the influence of release height on the deposited mass fraction

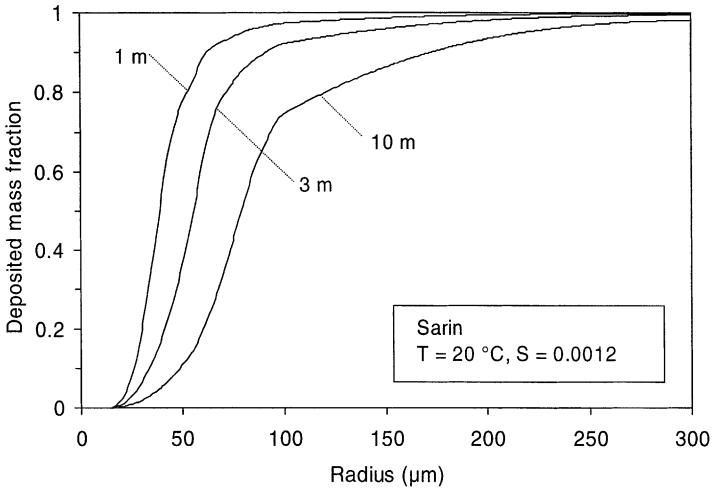

Fig. 6. The deposited mass fraction of a uniform population of sarin droplets against the initial droplet radius. The initial height of the volume is 1, 3 or 10 m. The gas temperature is 20°C and the vapour pressure of sarin in the gas is negligible.

of a population of sarin droplets. The droplet population is assumed to be monodisperse and uniformly distributed in a volume with the height of 1, 3 or 10 m. The droplet concentration is assumed to be low. Further, it is assumed that enough time is available for the process, i.e. finally all liquid sarin has either fallen to the ground or evaporated completely.

Clearly, the deposited mass fraction decreases with increasing release height, for all values of the initial droplet radius. A corresponding figure for a population of ammonia droplets has been presented by Vesala and Kukkonen [9]. The deposited mass fractions are substantially lower for ammonia, compared with those for sarin, due to the higher volatility of ammonia.

4. Conclusions

We have extended the model AERCLOUD (AERosol CLOUD) to treat two nerve agents, sarin and VX, and the mustard agent. This model evaluates the thermodynamical evolution of a five-component aerosol mixture, consisting of two-component droplets together with the surrounding three-component gas. This paper presents an overview of the model, and its extension to treat the above mentioned substances.

We have performed numerical computations regarding the evaporation and settling of airborne sarin droplets. We have defined a droplet radius r_M for which the drying time (total evaporation time) and the gravitational settling time are equal. This radius is a useful concept in deposition estimates. Droplets that are smaller than this size will evaporate totally while still airborne, whereas larger droplets will deposit on the ground before total evaporation takes place. The radii r_M range from approximately 15 to 80 μm for sarin droplets in the selected ambient conditions and initial heights. We have also evaluated the deposited mass fractions in terms of the initial droplet size.

Acknowledgements

We wish to thank Mr. Janne Koivukoski and Mr. Jukka Metso (Ministry of the Interior) for their cooperation. The authors are grateful for the financial support of the Scientific Committee for National Defence of Finland (MATINE). Our thanks are also due to Mr. Robin King for linguistic assistance with the manuscript.

Appendix A. The relevant physical and chemical properties of sarin, mustard agent and VX

The properties of sarin are estimated from the references Bryant et al. [20] and Reid et al. [21]; the properties of mustard agent and VX are estimated from the references Somani [3], Whitacre et al. [4], Prince [22], Ivarsson et al. [19], Reid et al. [21], Breck [23], Compton [24], Franke [25] and Watson et al. [26]. Table 1 presents a compilation of this data.

The binary diffusion coefficient D of sarin is $5.92 \times 10^{-6}\ m^2\ s^{-1}$. For mustard agent and VX, D is estimated from

$$D = 2.628 \times 10^{-7} \frac{\sqrt{(M_1 + M_2)(2M_1M_2)^{-1}}}{P\sigma_{12}^2 \Omega} T^{3/2} \quad \text{(A.1)}$$

Table 1
The physical and chemical properties of sarin, mustard agent and VX, relevant for source term and atmospheric dispersion computations[a]

Property	Substance	Value/equation	C_1	C_2	C_3	C_4
Molecular formula	Sarin	$C_4H_{10}FO_2P$				
	Mustard agent	$C_4H_8Cl_2S$				
	VX	$C_{11}H_{26}NO_2PS$				
Molecular weight (kg kmol^{-1})	Sarin	140.1				
	Mustard agent	159.08				
	VX	267.38				
Boiling point (K)	Sarin	424.65				
	Mustard agent	490				
	VX	571				
Critical temperature (K)[b]	Sarin	632.68				
	Mustard agent	724				
	VX	756				
Solubility (in water)	Sarin	Very soluble				
	Mustard agent	Soluble				
	VX	Soluble				
Polarity	Sarin	Polar				
	Mustard agent	Polar				
	VX	Polar				
Saturation vapour pressure (Pa)	Sarin	$p = 133.32 \exp(C_1 - C_2/T)$	23.2278	6679.83		
	Mustard agent		22.103	7255.446		
	VX		29.22	10930.37		
Vapour heat capacity (J (kg K)$^{-1}$)	Sarin	1911				
	Mustard agent	$4186\,(C_1 + C_2T + C_3T^2 + C_4T^3)/M$	10.7	9.36×10^{-2}	-4.64×10^{-5}	6.4×10^{-9}
	VX		12.2	0.247	-0.77×10^{-4}	-0.126×10^{-7}
Liquid heat capacity (J (kg K)$^{-1}$)	Sarin	2253				
	Mustard agent	1381				
	VX	1928				
Liquid density (kg m^{-3})	Sarin	$C_1 + C_2T + C_3T^2 + C_4T^3$	1428.5	−1.1017	-1.2224×10^{-4}	-2.3057×10^{-8}
	Mustard agent	$1000\,C_1C_2^{-(1-T_r)^{2/7}}$	1.093×10^{-2}	4.007×10^{-3}		
	VX		0.275	0.224		

Latent heat of vaporisation					
($J\,kg^{-1}$)	Sarin	$3.35{\cdot}10^5$ ($T = 25^\circ C$)			
	Mustard agent	$3.93{\cdot}10^5$ ($T = 25^\circ C$)			
	VX	$3.27{\cdot}10^5$ ($T = 25^\circ C$)			
Vapour thermal conductivity					
($J\,(s\,m\,K)^{-1}$)	Sarin	$C_1 + C_2T$	1.9042	-5.116×10^{-3}	
	Mustard agent		-1.873×10^{-3}	7.1×10^{-5}	
	VX		-6.923×10^{-3}	9.755×10^{-5}	
Vapour viscosity					
($kg\,(ms)^{-1}$)	Sarin	$C_1(T/T_0)^{C_2}$ ($T_0 = 273.15\,K$)	2.2461×10^{-3}	-5.4083	
	Mustard agent		1.538×10^{-5}	0.497	
	VX		1.307×10^{-5}	0.5	
Surface tension					
($N\,m^{-1}$)	Sarin	$0.001\,(C_1 + C_2t + C_3t^2)$ $[t] = ^\circ C$	28.713	-0.112	-6.6043×10^{-18}
	Mustard agent	$4.12{\cdot}10^{-4}$ ($T = 25^\circ C$)			
	VX	0.025 ($T = 25^\circ C$)			

[a] The parameters C_i ($i = 1, 2, 3, 4$) are the constant values in equations in the third column.

[b] The phosphorus atom is not included in estimating the critical temperature of VX.

where M_i is the molecular weight of species i, P the pressure in atmospheres and T the temperature. The collision integral Ω and σ_{12} are given by

$$\Omega = \frac{1.06036}{T^{*0.1561}} + \frac{0.193}{\exp(0.47635T^*)} + \frac{1.03587}{\exp(1.52996T^*)} + \frac{1.76474}{\exp(3.89411T^*)} \quad (A.2)$$

$$\sigma_{12} = \frac{\sigma_1 + \sigma_2}{2} \quad (A.3)$$

where $T^* = T\,k/(\varepsilon_1\,\varepsilon_2)^{1/2}$, where k is Boltzmann's constant and ε_i is the Lennard–Jones energy of species i, which is estimated by $\varepsilon_i = 1.15\,k\,T_{bi}$, where T_{bi} is the boiling point of species i. The Lennard–Jones length σ_i of species i is estimated by $\sigma_i = 0.118\,(M_i/\rho_{bi})^{1/3}$, where ρ_{bi} is the density of liquid at boiling point and σ_2 is 6.36 Å and 7.93 Å for mustard agent and VX, respectively.

The molecular structure of these compounds is as follows.

Sarin:

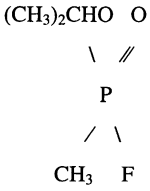

Mustard agent: $ClCH_2CH_2–S–CH_2CH_2Cl$

VX:

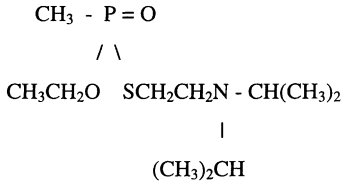

References

[1] G.H. Milly, S.D. Thayer, Techniques for Dosage Prediction, Vol. I, Development of Techniques, US Army Dugway Proving Ground, Dugway, Utah, USA, 1967, p. 439 + app.

[2] M.C. Johnson, Methodology for Chemical Hazard Prediction, Department of Defence Explosives Safety Board, Alexandria, Virginia, USA, 1980, p. 22 + app.

[3] S.M. Somani (Ed.), Chemical Warfare Agents, Academic Press, San Diego, 1992, p. 443.

[4] C.G. Whitacre, J.H. Griner III, M.M. Myirski, D.W. Sloop, Personal Computer Program for Chemical Hazard Prediction (D2PC), CRDEC TR-87021, US Army Armament Munitions Chemical Command, Chemical Research, Development and Engineering Center, Aberdeen Proving Ground, Maryland, 1987, p. 25 + app.

[5] J. Aroesty, Atmospheric Diffusion of Droplet Clouds, Report RAND/N-2134-ARPA RAND Corporation, Santa Monica, CA, USA, 1984, p. 25.

[6] US Army, Handbook for Chemical Hazard Prediction, United States Army Material Development and Readiness Command, Alexandria, 1980.

[7] V.M. Kolodkin, Risk assessments of the potential hazard connected with the objects of storage of warfare chemical agents, in: F.W. Holm (Ed.), Effluents from Alternative Demilitarisation Technologies, Kluwer Academic Publishers, The Netherlands, 1998, pp. 121–139.
[8] J. Kukkonen, T. Vesala, M. Kulmala, The interdependence of evaporation and settling for airborne freely falling droplets, J. Aerosol Sci. 20 (7) (1989) 749–763.
[9] T. Vesala, J. Kukkonen, A model for binary droplet evaporation and condensation, and its application for ammonia droplets in humid air, Atm. Environ. 26A (1992) 1573–1581.
[10] J. Nikmo, J. Kukkonen, T. Vesala, M. Kulmala, A model for mass and heat transfer in an aerosol cloud, J. Hazard. Mater. 38 (1994) 293–311.
[11] T. Vesala, J. Kukkonen, M. Kulmala, A Model for evaporation of freely falling droplets, Finnish Meteorological Institute, Publications on Air Quality 6, Helsinki, 1989, p. 58.
[12] T. Vesala, Binary Droplet Evaporation and Condensation as Phenomenological Processes, Ph.D. thesis, University of Helsinki Commentationes Physico-Mathematicae 127, The Finnish Society of Sciences and Letters, Helsinki, 1991, p. 104.
[13] J. Kukkonen, M. Kulmala, J. Nikmo, T. Vesala, D.M. Webber, T. Wren, The homogeneous equilibrium approximation in models of aerosol cloud dispersion, Atm. Environ. 28 (1994) 2763–2776.
[14] M. Kulmala, T. Vesala, Condensation in the continuum regime, J. Aerosol Sci. 22 (3) (1991) 337–346.
[15] C.F. Curtiss, J.O. Hirschfelder, Transport properties of multicomponent gas mixtures, J. Chem. Phys. 17 (6) (1949) 550–555.
[16] R.B. Bird, W.E. Stewart, E.N. Lightfoot, Transport phenomena, Wiley, New York, 1960.
[17] J.H. Seinfeld, Atmospheric Chemistry and Physics of Air Pollution, Wiley/Interscience, New York, 1986.
[18] P.E. Wagner, F.G. Pohl, The interdependence of droplet growth and concentration I. Theory of droplet growth and applications on condensation nuclei counters, J. Colloid Interf. Sci. 53 (1975) 429–438.
[19] U. Ivarsson, H. Nilsson, J. Santesson (Eds.), A FOA Briefing Book on Chemical Weapons, Threat, Effects and Protection, Försvarets forskningsanstalt (FOA), Sundbyberg, Sweden, 1992, p. 77.
[20] P.J.R. Bryant, A.H. Ford-Moore, B.J. Perry, A.W.H. Wardrop, T.F. Watkins, The preparation and physical properties of isopropyl methylphosphonofluoridate (sarin), J. Chem. Soc. (1960) 1553–1555.
[21] R.C. Reid, J.M. Prausnitz, B.E. Poling, The Properties of Gases and Liquids, 4th Edition, McGraw-Hill, New York, 1986, p. 741.
[22] A.J. Prince, The DATABANK — A computer program for evaluating the physical properties of hazardous vapours, United Kingdom Atomic Energy Authority, SRD R 499, Warrington, 1990, p. 19.
[23] J.E. Breck, Behavior of chemical warfare agents in water: aquatic transport modelling for assessing the potential impacts of accidental releases, Environ. Professional 11 (4) (1989) 324–334.
[24] J.A.F. Compton, Military chemical and biological agents: chemical and toxicological properties, The Telford Press, Caldwell, NJ, 1987, p. 458.
[25] S. Franke, Lehrbuch der Militärchemie Band 1, Deutscher Militärverlag, Berlin, 1967, p. 542.
[26] A.P. Watson, K.R. Ambrose, G.D. Griffin, S.S. Leffingwell, N.B. Munro, L.C. Waters, Health effects of warfare agent exposure: implications for stockpile disposal, Environ. Professional 11 (4) (1989) 335–353.